Nonsequential Double Ionization by Counterrotating Circularly Polarized Two-Color Laser Fields

S. Eckart,[1] M. Richter,[1] M. Kunitski,[1] A. Hartung,[1] J. Rist,[1] K. Henrichs,[1] N. Schlott,[1] H. Kang,[1,2] T. Bauer,[1] H. Sann,[1] L. Ph. H. Schmidt,[1] M. Schöffler,[1] T. Jahnke,[1] and R. Dörner[1,*]

[1]*Institut für Kernphysik, Goethe-Universität, Max-von-Laue-Straße 1, 60438 Frankfurt, Germany*

[2]*State Key Laboratory of Magnetic Resonance and Atomic and Molecular Physics, Wuhan Institute of Physics and Mathematics, Chinese Academy of Sciences, Wuhan 430071, China*

(Received 1 June 2016; published 20 September 2016)

We report on nonsequential double ionization of Ar by a laser pulse consisting of two counterrotating circularly polarized fields (390 and 780 nm). The double-ionization probability depends strongly on the relative intensity of the two fields and shows a kneelike structure as a function of intensity. We conclude that double ionization is driven by a beam of nearly monoenergetic recolliding electrons, which can be controlled in intensity and energy by the field parameters. The electron momentum distributions show the recolliding electron as well as a second electron which escapes from an intermediate excited state of Ar^+.

DOI: 10.1103/PhysRevLett.117.133202

Strong laser fields efficiently lead to the ejection of electrons from atoms and molecules. In the continuum, the electron wave packet is driven by the laser field, and its trajectory can be controlled by tailoring the time evolution of the electric field vector of the laser pulse on a subcycle basis. A laser pulse composed of two harmonic colors already offers a significant amount of control parameters, such as polarization, relative intensity, and phase between the two fields. This allows us to shape the light field and thus to steer the electron motion in the continuum or in a bond [1–9]. Particularly versatile and in addition well controllable waveforms are generated by counterrotating circular two-color (CRTC) fields shown in Figs. 1(c), 1(f), and 1(i). These waveforms have spawned recent activities because, unlike single-color circularly polarized light, CRTC fields can initially drive electrons away from the atom but later drive them back—often on triangularly shaped trajectories to reencounter their parent ion. The recapture of these electrons gives rise to the emission of circularly polarized higher harmonic light as predicted in pioneering work by Becker *et al.* [10] and confirmed by recent experimental studies [11]. The recollision in such fields has also been identified by high energetic electrons [12] and characteristic structures in the electron momentum distribution at very low energies [13].

In the present work, we experimentally show that CRTC fields also lead to efficient double ionization mediated by the recolliding electron as predicted by recent classical ensemble calculations [14]. Studying the probability of double ionization and the three-dimensional momentum distribution of the emitted electrons gives unprecedented insight into the recollision dynamics occurring in these two-color laser fields. They support that CRTC fields can be used to create a nearly monoenergetic electron beam for attosecond time-resolved studies. Additionally, very recent theoretical work [15] building on Ref. [16] predicts that these recolliding electrons can be generated such that they are spin polarized [17].

In order to generate two-color fields, we use a 200-μm β-barium borate crystal to frequency double a 780-nm laser pulse (KMLabs Dragon, 40-fs FWHM, 8 kHz). The fundamental and the second harmonic are separated using a dielectric beam splitter. Before the two are recombined and focused (spherical mirror, $f = 80$ mm), a neutral density filter, followed by a $\lambda/2$ and a $\lambda/4$ wave plate, is installed in each pathway. In the arm of the fundamental wavelength, a nm-delay stage is used to adjust the temporal overlap (relative phase) between the two colors [3]. The laser field is focused into an argon target that is generated using supersonic gas expansion. The peak intensity in the focus was calibrated separately for both colors using the photoelectron momentum distributions from ionization by circularly polarized light. For 780 mm, the intensity in the focus was obtained from the measured drift momentum. For 390 mm, we observed clear peaks in the photoelectron energy distribution spaced by the photon energy. We used the shift of the energy of these peaks as a function of intensity, which is due to the change in ponderomotive energy, for calibration of the intensity in the focus. The uncertainty of the absolute intensity for 780 and 390 mm is estimated to be 10% and 20%, respectively. It should be noted that our intensity calibration is an *in situ* measurement of the electric field and hence includes focal averaging for single ionization. To minimize the effect of focal averaging, the gas jet was collimated to 40 ± 10 μm along the axial direction in the laser focus (Rayleigh length of about 150 mm) for all measurements except the data presented in Fig. 2.

The three-dimensional electron momenta presented in this Letter have been measured in coincidence with argon

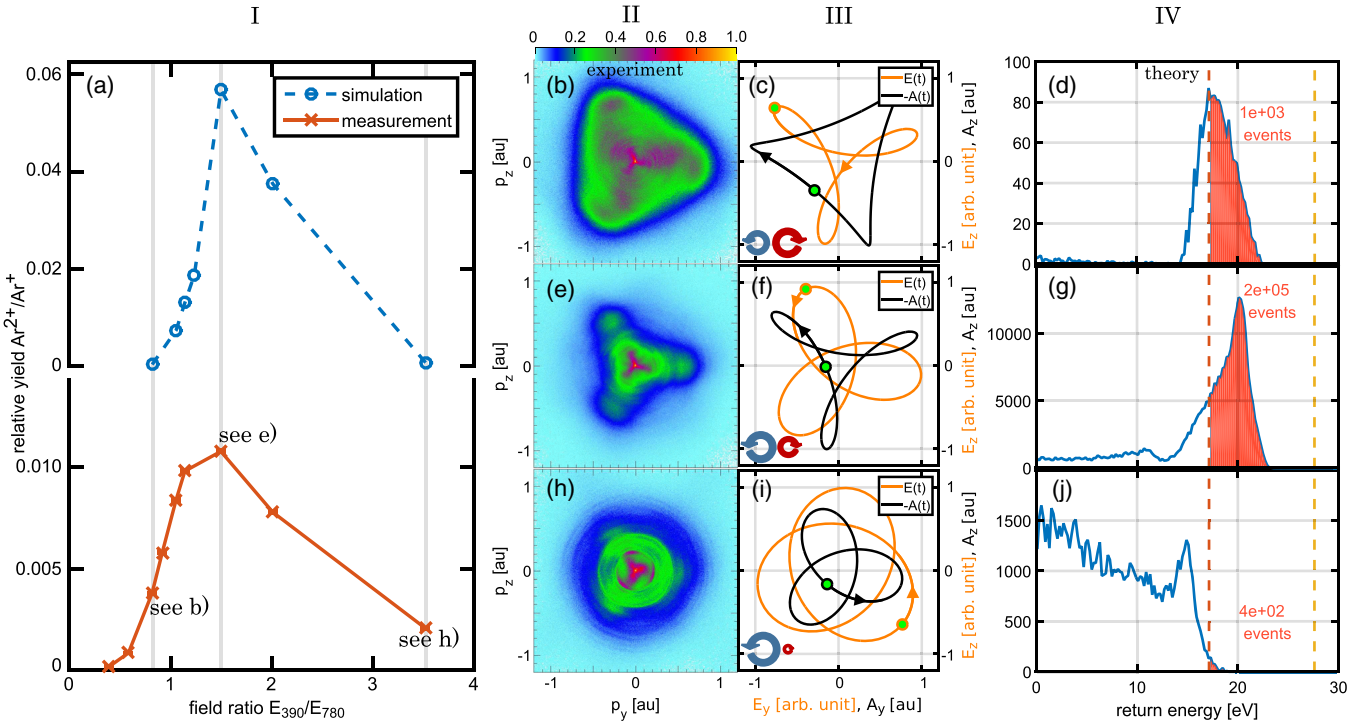

FIG. 1. The measured and simulated relative yield of double to single ionization is shown in column I. In column II, measured electron momentum distributions are shown for the field ratios E_{390}/E_{780} of (b) 0.8:1, (e) 1.5:1, and (h) 3.5:1 and a maximum combined intensity of 5.0×10^{14} W/cm^2. In column III, the corresponding combined electric fields E_y and E_z (arbitrary units) as well as the vector potentials A_y and A_z (atomic units) are depicted for the same ratios E_{390}/E_{780} (c) 0.8:1, (f) 1.5:1, and (i) 3.5:1. One maximum of the combined electric field is marked with a green dot. The helicities and the temporal development of the electric fields and the vector potentials are indicated with arrows. In column IV, the corresponding simulated energy distribution of the returning electrons is shown, which has been calculated also for the ratios E_{390}/E_{780} (d) 0.8:1, (g) 1.5:1, and (j) 3.5:1 using CTMC simulations. The energy needed for double ionization (27.6 eV) and the relevant excitation energy (17.14 eV) are marked with dashed orange and red lines, respectively. The number of recollision events is normalized to 10^6 single-ionization events in column IV. All events exceeding 17.14 eV are integrated, which is visualized as the shaded red area. This integral corresponds to the number of returning electrons having enough energy to excite Ar^+ and strongly depends on the field ratio E_{390}/E_{780}.

ions using cold-target recoil-ion momentum spectroscopy [18]. The lengths of the electron and ion arms were 378 and 67.8 mm, respectively. The homogeneous electric and magnetic fields of 11.2 V cm^{-1} and 8.3 G, respectively, guided electrons and ions towards position sensitive microchannel plate detectors with three layer delay-line anodes [19]. Only one electron was measured for single- and double-ionization events.

Using momentum conservation as a criterion, the false electron-ion coincidences for the single ionization of argon resulting from simultaneous ionization of two different atoms in one laser shot are determined to be 25%. This leads to 14% of the electrons that are detected in coincidence with Ar^{2+} to stem from the simultaneous single ionization of a second atom. We have corrected our measured electron momentum distributions for these false coincidences.

In Fig. 1(a), we show the ratio of doubly to singly charged argon ions as function of the relative field strength E_{390}/E_{780} of the 780- and 390-mm fields. The corresponding photoelectron distributions in Figs. 1(b), 1(e), and 1(h) are presented along with combined electric fields and vector potentials in Figs. 1(c), 1(f), and 1(i) for three selected field ratios. The maximum combined electric field amplitude corresponds to an intensity of 5.0×10^{14} W/cm^2. To characterize the strength of the different combined fields, we use equivalent intensities, which ensures that the single-ionization rate for given equivalent intensities is similar for different shapes of the field. We find that the double-ionization probability depends strongly on the relative intensity of the two colors confirming a recent prediction [14]. The double-ionization probability shows a maximum at the ratio $E_{390}/E_{780} = 1.5$. Double ionization vanishes for purely circular light, which is clear evidence that double ionization takes place nonsequentially and is mediated by recollision.

To illuminate the recollision physics causing the observed dependence of double-ionization probability, we show the measured electron momentum distributions for single ionization (Fig. 1, column II) together with the simulated energy distributions of recolliding electrons (Fig. 1, column IV). The measured electron momentum

distributions exhibit a strong dependence on E_{390}/E_{780} in qualitative agreement with recent reports [6,12]. Column IV in Fig. 1 shows simulated energy distributions of recolliding electrons at the distance of closest approach using a classical trajectory Monte Carlo (CTMC) simulation. For this, we have calculated classical electron trajectories with weights obtained by Ammosov-Delone-Krainov theory [20] starting at the exit of the tunnel with zero momentum in the direction parallel to the tunnel and a Gaussian distribution of momenta transverse to the tunnel direction. The electron trajectories are calculated in the presence of the Coulomb field. In order to select trajectories which potentially can lead to ionization or excitation of the parent ion, we have postselected electrons, which have passed the parent ion at a distance smaller than $d_{\min} = 5$ a.u., and have plotted their excess energy at the instant of closest approach. The number of trajectories has been normalized to the total number of 10^6 freed electrons and thus gives the fraction compared to total single ionization. Also indicated in Fig. 1 (column IV) are the energy of the first relevant excited state of Ar^+ at 17.14 eV and the ionization threshold at 27.6 eV. Strikingly, the distributions of recollision energies shows a pronounced narrow peak, which is swept in energy and intensity as the ratio E_{390}/E_{780} is varied. The measured maximum of the double-ionization yield [Fig. 1(a)] coincides with the field ratio, for which the flux of recolliding electrons with energies sufficient to excite the Ar^+ reaches its maximum. At the intensities used in the experiment, there are no recolliding electrons with energies above the Ar^+ ionization threshold (dashed yellow line in Fig. 1, column IV). This suggests that double ionization occurs solely by recollision induced excitation followed by subsequent ionization of Ar^{+*} (see, e.g., Refs. [21–23]).

To model the double-ionization yield by impact excitation more quantitatively, we have weighted the simulated electron energy distributions shown in Figs. 1(d), 1(g), and 1(j) with the energy-dependent electron impact excitation cross section from Ref. [24] and integrated over the electron energy. This simple estimate reproduces the observed E_{390}/E_{780} dependence of double ionization as shown by the dashed line in Fig. 1(a). Although the obtained maximum turned out to be robust regarding the choice of $d_{\min}$, it should be noted that the somewhat arbitrary value of $d_{\min}$ as a selection criterion of the recollision trajectory allows us to estimate only the dependence of the double-ionization yield on E_{390}/E_{780} but not an absolute value as, for example, given by quantitative rescattering theory [25].

So far, our scan of E_{390}/E_{780} together with the trajectory simulations suggests that double ionization in CRTC fields is driven by recollision induced excitation and that tuning E_{390}/E_{780} allows us to create nearly monoenergetic beams of recolliding electrons [see Figs. 1(d) and 1(g)]. To further support and detail these findings, we discuss in the remainder of this Letter the intensity dependence of double ionization in CRTC fields and compare the three-dimensional momentum distribution of the electrons from single and double ionization.

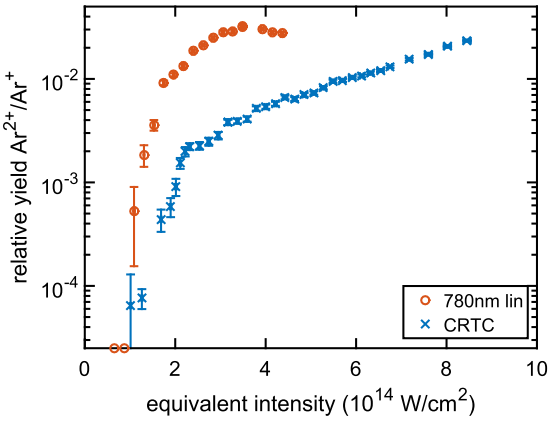

FIG. 2. Relative yield of double ionization is shown as a function of intensity in focus for linear polarization at 780 mm and for a CRTC field with $E_{390}/E_{780} = 1.23$, which is close to the maximum in Fig. 1(a). For the CRTC field, a similar kneelike shape is observed as it is commonly known for linear polarization. The two first points for linear polarization on the ordinate indicate that no double-ionization events were measured within a reasonable amount of time.

Figure 2 shows the intensity dependence of the $Ar^{2+}:Ar^+$ ratio for a CRTC field with $E_{390}/E_{780} = 1.23$, which is close to the maximum in Fig. 1(a). We have found a steep increase of double ionization at an intensity of around 2.0×10^{14} W/cm^2 followed by a broad plateau. This shape is very similar to the kneelike shape for linear polarized light (red circles) (see, e.g., Ref. [26]). The double-ionization probability of the CRTC fields is suppressed by 1 order of magnitude. The reason for this suppression is that in contrast to linearly polarized light, the electrons in CRTC fields are driven in two dimensions, and hence they often require some initial momentum in order to recollide with the core. This is similar to the double-ionization suppression for elliptically polarized light or orthogonal linearly polarized two-color fields [2]. An inspection of the energy of simulated recollision electrons confirms that the sharp dropoff of double ionization below 2.0×10^{14} W/cm^2 is caused by an absence of recolliding electrons with energies above the first relevant excitation energy of Ar^+.

To further illuminate the double-ionization dynamics in the CRTC fields, we have measured the electron momentum distribution for double ionization [Fig. 3(b)]. First inspection shows significantly higher momenta and a counterclockwise rotation of the triangular structure for electrons from double ionization as compared to those from single ionization [Fig. 3(a)]. The counterclockwise rotation is caused by the increase of the influence of the Coulomb potential for the doubly charged as compared to the singly charged ion. Single-ionization electrons freed at the

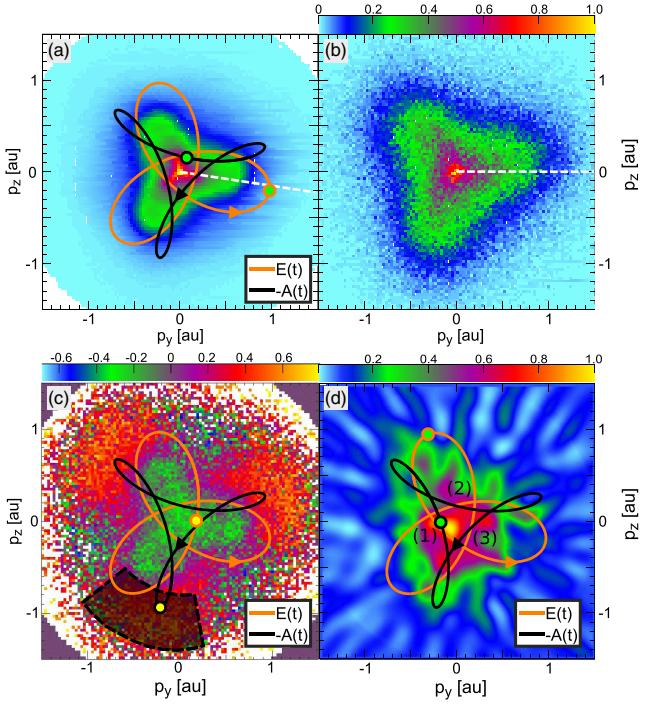

FIG. 3. Measured electron momentum distributions for (a) single and (b) double ionization for a ratio of $E_{390}/E_{780} = 1.42$ and a combined intensity of 4.5×10^{14} W/cm^2. The corresponding vector potential is shown as a black curve, and the phase that belongs to the maximum combined field is indicated by a green dot. The dashed white line serves as guide to the eye regarding the rotation of the low-energy structure (purple structure at momenta smaller than 0.3 a.u.). (c) The normalized difference $(A-B)/(A+B)$ where A (B) is the number of counts in the corresponding bins normalized to the sum of all counts for double (single) ionization. (d) The tomographically reconstructed electron momentum distribution is shown for the condition that the first electron has been detected in the shaded area in (c). Electrons in this area have recollisionally excited the ion at the time of the pulse which is indicated by the yellow dot in (c). In (d), we show the momenta of the corresponding excited electron set free later in the pulse. The labels 1, 2, and 3 represent the first (1), second (2), and third (3) maxima of the field following the recollision and correspond to time delays of 433, 1300, and 2167 attoseconds after recollision.

maximum of the field with zero energy would in the absence of the Coulomb potential be streaked to a final momentum, which is given by the negative vector potential (green dot on the black line). We have taken the rotation angle of the Lissajous curve relative to our measured electron momentum distribution from time-dependent Schrödinger equation (TDSE) calculations [12] and our CTMC simulations.

From our arguments given in the discussion of Fig. 1, we expect two classes of electrons for double ionization: the initial electron, which recollides and creates an excitation, and the second electron, which is freed from the excited state later on in the laser field. The recolliding electron can be best seen in the data by calculating the normalized differences of the momentum distribution from double and single ionization [Fig. 3(c)]. The yellow-reddish area at the three tips of the vector potential in Fig. 3(c) results from these recolliding electrons. The feature spreads by 0.4–0.5 a.u. around the vector potential, indicating an electron momentum after rescattering which is in agreement with an energy excess of 3 eV left on the electron after excitation, which can be seen along the laser field free direction (p_x) in Fig. 3(d) at $p_x = 0.4$–0.5 a.u. as yellow-reddish distribution.

From the location of this feature close to the maximum of the vector potential [marked with a yellow dot in Fig. 3(c)], we conclude that the main contribution results from recollisions close to the electric field minimum. The second electron, which is set free at a subsequent maximum of the electric field [corresponding to a minimum of the vector potential and marked with a green dot in Figs. 3(a) and 3(d)], can be expected to have a momentum distribution similar to that of single ionization, with the main difference being that it shows a bigger Coulomb effect escaping from a doubly charged ion. Also, this is clearly seen in the data, as the inner threefold structure in Fig. 3(b) is rotated counterclockwise compared to the one from single ionization in Fig. 3(a). The rotation is indicated to the eye by the dashed white line (see, e.g., Ref. [27]).

In the next step, we now investigate the time delay between the recollisional excitation and emission of the excited electron. To do so, we impose the condition that the detected electron's momentum is in the gray shaded area in Fig. 3(c); we know that those electrons are mainly recolliding electrons. This sets the time at 0 for our time measurement. For technical reasons, such as detector dead time and poor ion momentum resolution in the two spatial dimensions, we have used a filtered back-projection algorithm to tomographically reconstruct the momentum distribution [6,12,28] of the second electron from the sum of the momenta of the first electron and the ion in the z direction as well as the relative phase of the two colors (which determines the rotation of the combined electric field in space). High frequencies are cut off in frequency space. The result is shown in Fig. 3(d). It can be nicely seen that the second electron is ionized close to the first [marked with (1) in Fig. 3(d)] maximum of the electric field about 433 attoseconds after the recolliding electron has hit the ion. At the second field maximum [label (2)], the electron flux is already reduced, and by the time of the third maximum, after 2 167 attoseconds, only a small fraction of excited electrons is left. This is a powerful example of how to use CRTC fields to study electron-emission dynamics on the attosecond time scale without being limited to near-single-cycle laser pulses (see, e.g., Ref. [29]).

In conclusion, we have shown that CRTC fields support nonsequential double ionization and at the same time allow for a detailed control of the energy distribution and direction of the recolliding electron wave packet. These

recolliding electron wave packets moving in CRTC fields have exciting applications. One is their use for the generation of higher harmonics with circular polarization, which is exploited already today [11]. Another possible application is the use of these wave packets to induce molecular dynamics by recollision [30], where the CRTC field would allow us to manipulate the energy and the direction from which the electron wave packet approaches the molecule. For such applications, it is particularly useful that due to the shape of the vector potential, the rescattered electrons are driven to an otherwise mainly empty region of momentum space, as demonstrated by our measurement. Yet another exciting future application builds on the fact that at the time, the electron is set free the field vector rotates as in circularly polarized light. This rotation gives rise to spin polarization of the emitted electrons [16,17]. Our study shows that CRTC fields are highly efficient to generate such electrons for electron impact ionization or excitation paving the way for attosecond time-resolved collision studies with spin-polarized electrons [15].

This work was supported by the DFG Priority Programme "Quantum Dynamics in Tailored Intense Fields." We thank Xiao-Min Tong for providing results from his TDSE calculations in numerical form.

Note added in proof.—Very recently the dependence of double ionization on the field ratio of two color fields was independently shown by Mancuso et al. [31].

*doerner@atom.uni-frankfurt.de

[1] M. Kitzler and M. Lezius, Spatial Control of Recollision Wave Packets with Attosecond Precision, Phys. Rev. Lett. **95**, 253001 (2005).

[2] L. Zhang, X. Xie, S. Roither, Y. Zhou, P. Lu, D. Kartashov, M. Schöffler, D. Shafir, P. B. Corkum, A. Baltuška *et al.*, Subcycle Control of Electron-Electron Correlation in Double Ionization, Phys. Rev. Lett. **112**, 193002 (2014).

[3] M. Richter, M. Kunitski, M. Schöffler, T. Jahnke, L. P. H. Schmidt, M. Li, Y. Liu, and R. Dörner, Streaking Temporal Double-Slit Interference by an Orthogonal Two-Color Laser Field, Phys. Rev. Lett. **114**, 143001 (2015).

[4] J. Geng, W. Xiong, X. Xiao, L. Peng, and Q. Gong, Nonadiabatic Electron Dynamics in Orthogonal Two-Color Laser Fields with Comparable Intensities, Phys. Rev. Lett. **115**, 193001 (2015).

[5] N. Douguet, A. N. Grum-Grzhimailo, E. V. Gryzlova, E. I. Staroselskaya, J. Venzke, and K. Bartschat, Photoelectron angular distributions in bichromatic atomic ionization induced by circularly polarized VUV femtosecond pulses, Phys. Rev. A **93**, 033402 (2016).

[6] C. Mancuso, D. D. Hickstein, P. Grychtol, R. Knut, O. Kfir, X. M. Tong, F. Dollar, D. Zusin, M. Gopalakrishnan, C. Gentry, E. Turgut, J. L. Ellis, M. Chen, A. Fleischer, O. Cohen, H. C. Kapteyn, and M. M. Murnane, Strong-field ionization with two-color circularly polarized laser fields, Phys. Rev. A **91**, 031402 (2015).

[7] L. Medišauskas, J. Wragg, H. van der Hart, and M. Y. Ivanov, Generating Isolated Elliptically Polarized Attosecond Pulses Using Bichromatic Counterrotating Circularly Polarized Laser Fields, Phys. Rev. Lett. **115**, 153001 (2015).

[8] E. Hasović, W. Becker, and D. B. Milošević, Electron rescattering in a bicircular laser field, Opt. Express **24**, 6413 (2016).

[9] K. Lin, X. Gong, Q. Song, Q. Ji, W. Zhang, J. Ma, P. Lu, Haifeng Pan, J. Ding, H. Zeng, and J. Wu, Directional bond breaking by polarization-gated two-color ultrashort laser pulses, J. Phys. B **49**, 025603 (2016).

[10] W. Becker, B. N. Chichkov, and B. Wellegehausen, Schemes for the generation of circularly polarized high-order harmonics by two-color mixing, Phys. Rev. A **60**, 1721 (1999).

[11] A. Fleischer, O. Kfir, T. Diskin, P. Sidorenko, and O. Cohen, Spin angular momentum and tunable polarization in high-harmonic generation, Nat. Photonics **8**, 543 (2014).

[12] C. Mancuso, D. D. Hickstein, K. M. Dorney, J. L. Ellis, E. Hasović, R. Knut, P. Grychtol, C. Gentry, M. Gopalakrishnan, D. Zusin *et al.*, Controlling electron-ion rescattering in two-color circularly polarized femtosecond laser fields, Phys. Rev. A **93**, 053406 (2016).

[13] T. Brabec, M. Y. Ivanov, and P. B. Corkum, Coulomb focusing in intense field atomic processes, Phys. Rev. A **54**, R2551 (1996).

[14] J. L. Chaloupka and D. D. Hickstein, Dynamics of Strong-Field Double Ionization in Two-Color Counterrotating Fields, Phys. Rev. Lett. **116**, 143005 (2016).

[15] D. B. Milošević, Possibility of introducing spin into atto-science with spin-polarized electrons produced by a bichromatic circularly polarized laser field, Phys. Rev. A **93**, 051402 (2016).

[16] I. Barth and O. Smirnova, Spin-polarized electrons produced by strong-field ionization, Phys. Rev. A **88**, 013401 (2013).

[17] A. Hartung, F. Morales, M. Kunitski, K. Henrichs, A. Laucke, M. Richter, T. Jahnke, A. Kalinin, M. Schöffler, L. P. H. Schmidt *et al.*, Electron spin polarization in strong-field ionization of xenon atoms, Nat. Photonics **10**, 526 (2016).

[18] J. Ullrich, R. Moshammer, A. Dorn, R. Dörner, L. P. H. Schmidt, and H. Schmidt-Böcking, Recoil-ion and electron momentum spectroscopy: Reaction-microscopes, Rep. Prog. Phys. **66**, 1463 (2003).

[19] O. Jagutzki, A. Cerezo, A. Czasch, R. Dörner, M. Hattas, M. Huang, V. Mergel, U. Spillmann, K. Ullmann-Pfleger, T. Weber *et al.*, Multiple hit readout of a microchannel plate detector with a three-layer delay-line anode, IEEE Trans. Nucl. Sci. **49**, 2477 (2002).

[20] N. B. Delone and V. P. Krainov, Energy and angular electron spectra for the tunnel ionization of atoms by strong low-frequency radiation, J. Opt. Soc. Am. B **8**, 1207 (1991).

[21] T. Weber, H. Giessen, M. Weckenbrock, G. Urbasch, A. Staudte, L. Spielberger, O. Jagutzki, V. Mergel, M. Vollmer, and R. Dörner, Correlated electron emission in multiphoton double ionization, Nature (London) **405**, 658 (2000).

[22] B. Feuerstein, R. Moshammer, D. Fischer, A. Dorn, C. D. Schröter, J. Deipenwisch, J. R. C. Lopez-Urrutia, C. Höhr, P. Neumayer, J. Ullrich *et al.*, Separation of Recollision

Mechanisms in Nonsequential Strong Field Double Ionization of Ar: The Role of Excitation Tunneling, Phys. Rev. Lett. **87**, 043003 (2001).

[23] Y. Liu, S. Tschuch, A. Rudenko, M. Dürr, M. Siegel, U. Morgner, R. Moshammer, and J. Ullrich, Strong-Field Double Ionization of Ar below the Recollision Threshold, Phys. Rev. Lett. **101**, 053001 (2008).

[24] V. L. B. De Jesus, B. Feuerstein, K. Zrost, D. Fischer, A. Rudenko, F. Afaneh, C. D. Schröter, R. Moshammer, and J. Ullrich, Atomic structure dependence of nonsequential double ionization of He, Ne and Ar in strong laser pulses, J. Phys. B **37**, L161 (2004).

[25] Z. Chen, A. T. Le, T. Morishita, and C. D. Lin, Quantitative rescattering theory for laser-induced high-energy plateau photoelectron spectra, Phys. Rev. A **79**, 033409 (2009).

[26] B. Walker, B. Sheehy, L. F. DiMauro, P. Agostini, K. J. Schafer, and K. C. Kulander, Precision Measurement of Strong Field Double Ionization of Helium, Phys. Rev. Lett. **73**, 1227 (1994).

[27] M. Spanner, S. Gräfe, S. Chelkowski, D. Pavičić, M. Meckel, D. Zeidler, A. B. Bardon, B. Ulrich, A. D. Bandrauk, D. M. Villeneuve, R. Dörner, P. B. Corkum, and A. Staudte, Coulomb asymmetry and sub-cycle electron dynamics in multiphoton multiple ionization of H_2, J. Phys. B **45**, 194011 (2012).

[28] C. Smeenk, L. Arissian, A. Staudte, D. M. Villeneuve, and P. B. Corkum, Momentum space tomographic imaging of photoelectrons, J. Phys. B **42**, 185402 (2009).

[29] B. Bergues, M. Kübel, N. G. Johnson, B. Fischer, N. Camus, K. J. Betsch, O. Herrwerth, A. Senftleben, A. M. Sayler, T. Rathje *et al.*, Attosecond tracing of correlated electron-emission in non-sequential double ionization, Nat. Commun. **3**, 813 (2012).

[30] X. Xie, K. Doblhoff-Dier, S. Roither, M. Schöffler, D. Kartashov, H. Xu, T. Rathje, G. G. Paulus, A. Baltuška, S. Gräfe *et al.*, Attosecond-Recollision-Controlled Selective Fragmentation of Polyatomic Molecules, Phys. Rev. Lett. **109**, 243001 (2012).

[31] C. A. Mancuso, K. M. Dorney, J. L. Chaloupka, J. L. Ellis, F. J. Dollar, R. Knut, P. Grychtol, D. Zusin, C. Gentry, H. C. Kapteyn, M. M. Murnane, and D. D. Hickstein, preceding Letter, Nonsequential Double Ionization in Two-Color Circularly Polarized Femtosecond Laser Fields, Phys. Rev. Lett. **117**, 133201 (2016).